

Decay and production properties of strange double charm pentaquark

Zi-Yan Yang^{1,2,3*} and Wei Chen^{4,5†}

¹*School of Mechanical Engineering and Robotic Engineering,*

Guangzhou City University of Technology, Guangzhou 510800, China

²*Key Laboratory of Atomic and Subatomic Structure and Quantum Control (MOE),*

Guangdong Basic Research Center of Excellence for Structure and Fundamental Interactions of Matter,

Institute of Quantum Matter, South China Normal University, Guangzhou 510006, China

³*Guangdong-Hong Kong Joint Laboratory of Quantum Matter,*

Guangdong Provincial Key Laboratory of Nuclear Science, Southern Nuclear Science Computing Center,

South China Normal University, Guangzhou 510006, China

⁴*School of Physics, Sun Yat-sen University, Guangzhou 510275, China and*

⁵*Southern Center for Nuclear-Science Theory (SCNT), Institute of Modern Physics, Chinese Academy of Sciences, Huizhou 516000, Guangdong Province, China*

In this work we investigate the decay and production properties of the strange double-charm pentaquark P_{ccs}^{++} with strangeness $S = -1$. Building upon our previous work predicting its $J^P = 1/2^-$ molecular configuration, we employ three-point QCD sum rules to calculate its strong decay widths and estimate its production branching ratios via Ξ_{bc}^+ baryon decays. The total strong decay width into the $\Xi_{cc}\bar{K}$ and $\Omega_{cc}\pi$ final-state channels is determined as $84.58^{+19.25}_{-18.80}$ MeV. Furthermore, using a rescattering mechanism, we analyze the $\Xi_{bc}^+ \rightarrow D_s^{*-}\Xi_{cc}^{++} \rightarrow D^-P_{ccs}^{++}$ process and estimate the production branching ratio to be $\mathcal{B}r(\Xi_{bc}^+ \rightarrow D^-P_{ccs}^{++}) = (4.32^{+2.02}_{-1.47}) \times 10^{-6}$. The relatively narrow width and detectable branching ratio suggest that this pentaquark state could be observed in experiments such as LHCb.

PACS numbers: 12.39.Mk, 12.38.Lg, 14.40.Ev, 14.40.Rt

Keywords: Pentaquark states, exotic states, QCD sum rules

I. INTRODUCTION

The study of exotic multi-quark states, proposed early in 1964 [1, 2], has become a pivotal frontier in hadronic physics, offering profound insights into the nonperturbative dynamics of quantum chromodynamics (QCD) [3–15]. Since the discovery of the first hidden-charm pentaquarks $P_c(4380)$ and $P_c(4450)$ by the LHCb Collaboration [16], significant theoretical and experimental efforts have been devoted to unraveling the nature of these states, which lie beyond the conventional quark model. The recent observation of the double-charm tetraquark $T_{cc}^+(3875)$ [17, 18] and the strange-charm tetraquark $T_{c\bar{s}}(2900)$ [19] further highlights the rich spectrum of exotic hadrons and underscores the potential existence of their double-heavy counterparts, such as double-charm pentaquarks.

Theoretical attempts have been made to study the mass spectrum from both the hadronic molecular picture [20–29] and the compact pentaquark picture [30–34], as well as their electromagnetic properties [28, 29, 35–38]. In our previous work [39], we systematically investigated the mass spectra of strange double-charm pentaquarks with quark content $ccus\bar{d}$ and strangeness $S = -1$, employing QCD sum rules for both molecular and compact configurations. Among the predicted configurations, the $J^P = 1/2^-$ molecular pentaquark with $\Xi_{cc}\bar{K}$ structure stands out: its mass (4.20 GeV) lies slightly above the $\Xi_{cc}\bar{K}$ threshold, allowing strong decays only into $\Xi_{cc}\bar{K}$ and $\Omega_{cc}\pi$ channels. This suggests a relatively narrow resonance that could manifest as a discernible peak in experimental invariant mass spectra. The proximity to the threshold suppresses the phase space for strong decays, potentially enhancing its experimental detectability.

Meanwhile, the ongoing experimental quest for doubly heavy Ξ_{bc}^+ baryons offers a pivotal opportunity to unravel the double-charm pentaquark state. Cabibbo-favored decays of Ξ_{bc}^+ , such as $\Xi_{bc}^+ \rightarrow D_s^{*-}\Xi_{cc}^{++}$, could generate the $\Xi_{cc}\bar{K}$ pentaquark through rescattering processes. At the quark level, the diagram for the process $\Xi_{bc}^+ \rightarrow D^-P_{ccs}^{++}$ is shown in the left panel of Fig. 1. The weak decay arises from a Cabibbo-favored weak transition $b \rightarrow c(\bar{c}s)$ along with the creation of a $d\bar{d}$ pair from the strong interaction. This diagram, known as the external W emission diagram, is non-factorizable because the $s\bar{c}$ pair produced in the weak interaction ends up in different final-state hadrons. Thus, long-distance contributions play a significant role in the

*Electronic address: yangzh@gcu.edu.cn

†Electronic address: chenwei29@mail.sysu.edu.cn

$\Xi_{bc}^+ \rightarrow D^- P_{ccs}^{++}$ process, where the weakly produced $c\bar{s}$ and ucc pairs hadronize as D_s^{*-} and Ξ_{cc}^{++} , respectively, followed by a strong rescattering between D^- and P_{ccs}^{++} mediated by \bar{K}^0 meson exchange. The corresponding rescattering process at the hadronic level is shown in the right panel of Fig. 1. The rescattering mechanism for final-state-interaction (FSI) effects has been successfully applied to D meson decays [40], B meson decays [41, 42], and charm baryon decays [43, 44]. Recently, this mechanism has also been applied to the production of tetraquark states in B meson decays [45, 46] and of hidden-charm pentaquark states P_c in Ξ_b decays [47]. In this work, we apply the rescattering mechanism to the production of the double-charm pentaquark via the $\Xi_{bc}^+ \rightarrow D_s^{*-} \Xi_{cc}^{++} \rightarrow D^- P_{ccs}^{++}$ process with \bar{K}^0 exchange.

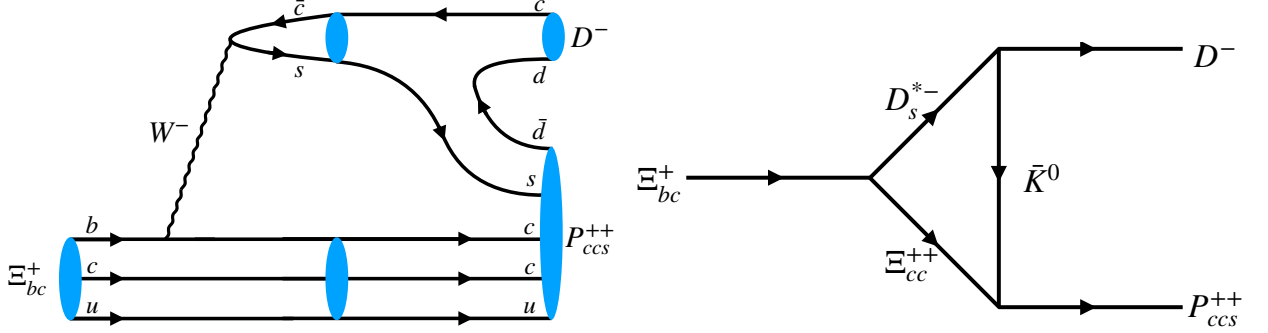


FIG. 1: The production of the strange double-charm pentaquark at the quark level (left) and hadronic level (right).

A precise calculation of the decay width and production branching ratios of the double-charm pentaquark is thus critical to quantify its production rates in such channels and to guide experimental searches at facilities like LHCb and Belle II. In this work, we continue our study by calculating the decay width of the double-charm pentaquark using the QCD sum rule method and estimating its production branching ratios in Ξ_{bc} decays. This paper is organized as follows: In Sec. II, we outline the formalism for computing decay widths within the QCD sum rule approach. Sec. III presents the numerical results for the $J^P = 1/2^-$ pentaquark's decay properties. Sec. IV discusses its production mechanism via Ξ_{bc}^+ decays and estimates detectable branching ratios. A brief summary is presented in Sec. V.

II. THREE POINT QCD SUM RULE

Over past several decades, the method of QCD sum rule has been proven to be very powerful to study hadron properties [48–51]. In this section, we shall study the three-point correlation function of several two-body strong decay process $M \rightarrow X + Y$. For the strong decay process $M \rightarrow X + Y$, the corresponding correlator is written as

$$\Pi(p, p', q) = \int d^4x d^4y e^{ip' \cdot x} e^{iq \cdot y} \langle 0 | T \{ J_X(x) J_Y(y) J_M^\dagger(0) \} | 0 \rangle, \quad (1)$$

where $J_{M(X,Y)}$ is the interpolating current for the initial(final) state. In this section, we shall consider the $P_{ccs} \Xi_{cc} \bar{K}$ and $P_{ccs} \Omega_{cc} \pi$ strong decay vertices with $K(\pi)$ off shell. We use the following interpolating currents for P_{ccs}^{++} by considering it as a $\Xi_{cc} \bar{K}$ molecule [39]:

$$\xi_1 = [\epsilon_{abc} (c_a^T C \gamma_\mu c_b) \gamma_\mu \gamma_5 u_c] [\bar{d}_d \gamma_5 s_d], \quad (2)$$

where C denote the charge conjugate operator, subscript $a \cdots d$ denote the color index and u, d, s, c denote the up, down, strange, charm quark field, respectively. These current can couple to the P_{ccs}^{++} state with $J^P = 1/2^-$ via

$$\langle 0 | \xi_1 | P_{ccs}^{1/2^-} \rangle = \lambda_{P_{ccs}}^- u(p), \quad (3)$$

in which the value of the coupling constant $\lambda_{P_{ccs}}^-$ are determined from the two-point mass sum rules established in Ref. [39]:

$$\lambda_{P_{ccs}}^- = (2.3 \pm 0.7) \times 10^{-3} \text{ GeV}^6. \quad (4)$$

The interpolating currents for \bar{K} and π^+ mesons can be constructed as

$$J_{\bar{K}} = i \bar{d}_a \gamma_5 s_a, \quad J_{\pi^+} = i \bar{d}_a \gamma_5 u_a, \quad (5)$$

which can coupling to the meson states via

$$\langle 0|J_{\bar{K}}|\bar{K}\rangle = f_{\bar{K}} \frac{m_{\bar{K}}^2}{m_s} \equiv \lambda_{\bar{K}}, \quad \langle 0|J_{\pi^+}|\pi^+\rangle = f_{\pi} \frac{m_{\pi}^2}{m_u + m_d} \equiv \lambda_{\pi}. \quad (6)$$

The interpolating currents for double charm baryons are taken as [52]

$$\begin{aligned} J_{\Xi_{cc}} &= \epsilon_{abc}(c_a^T C \gamma_{\mu} c_b) \gamma_{\mu} \gamma_5 u_c, \\ J_{\Omega_{cc}} &= \epsilon_{abc}(c_a^T C \gamma_{\mu} c_b) \gamma_{\mu} \gamma_5 s_c, \end{aligned} \quad (7)$$

which can coupling to the baryon states via

$$\begin{aligned} \langle 0|J_{\Xi_{cc}}|\Xi_{cc}(p, s)\rangle &= f_{\Xi_{cc}} u(p, s), \\ \langle 0|J_{\Omega_{cc}}|\Omega_{cc}(p, s)\rangle &= f_{\Omega_{cc}} u(p, s). \end{aligned} \quad (8)$$

The coupling constant $g_{P_{ccs}\Xi_{cc}\bar{K}}$ and $g_{P_{ccs}\Omega_{cc}\pi}$ are defined via the effective Lagrangian [53]

$$\begin{aligned} \mathcal{L}_{P_{ccs}\Xi_{cc}\bar{K}} &= g_{P_{ccs}\Xi_{cc}\bar{K}} P_{ccs} \bar{\Xi}_{cc} \bar{K}, \\ \mathcal{L}_{P_{ccs}\Omega_{cc}\pi} &= g_{P_{ccs}\Omega_{cc}\pi} P_{ccs} \bar{\Omega}_{cc} \bar{\pi}, \end{aligned} \quad (9)$$

thus the transition matrix element can be obtained as

$$\begin{aligned} \langle \Xi_{cc}(p', s') \bar{K}(q) | P_{ccs}(p) \rangle &= g_{P_{ccs}\Xi_{cc}\bar{K}} \bar{u}_{\Xi_{cc}}(p', s') u_{P_{ccs}}(p, s), \\ \langle \Omega_{cc}(p', s') \pi(q) | P_{ccs}(p) \rangle &= g_{P_{ccs}\Omega_{cc}\pi} \bar{u}_{\Omega_{cc}}(p', s') u_{P_{ccs}}(p, s). \end{aligned} \quad (10)$$

With the above coupling relations and transition matrix element, we can obtain the three-point correlation function Eq. (1) for $P_{ccs}^{++} \rightarrow \Xi_{cc}\bar{K}$ on the phenomenological side

$$\begin{aligned} \Pi(p, p', q) &= \int d^4x d^4y e^{ip' \cdot x} e^{-iq \cdot y} \langle 0 | T \{ J_{P_{ccs}}(x) J_{\bar{K}}^{\dagger}(y) J_{\Xi_{cc}}^{\dagger}(0) \} | 0 \rangle \\ &= \frac{\lambda_{P_{ccs}}^{-} \lambda_{\Xi_{cc}} \lambda_K g_{P_{ccs}\Xi_{cc}\bar{K}}}{(p^2 - m_{P_{ccs}}^2)(p'^2 - m_{\Xi_{cc}}^2)(q^2 - m_K^2)} (\not{p} + m_{P_{ccs}})(\not{p}' + m_{\Xi_{cc}}) + \dots, \end{aligned} \quad (11)$$

and for $P_{ccs}^{++} \rightarrow \Omega_{cc}\pi$ process

$$\begin{aligned} \Pi(p, p', q) &= \int d^4x d^4y e^{ip' \cdot x} e^{-iq \cdot y} \langle 0 | T \{ J_{P_{ccs}}(x) J_{\pi}^{\dagger}(y) J_{\Omega_{cc}}^{\dagger}(0) \} | 0 \rangle \\ &= \frac{\lambda_{P_{ccs}}^{-} \lambda_{\Omega_{cc}} \lambda_K g_{P_{ccs}\Omega_{cc}\pi}}{(p^2 - m_{P_{ccs}}^2)(p'^2 - m_{\Omega_{cc}}^2)(q^2 - m_{\pi}^2)} (\not{p} + m_{P_{ccs}})(\not{p}' + m_{\Omega_{cc}}) + \dots, \end{aligned} \quad (12)$$

On the OPE side, we can evaluate the correlation function with standard QCD sum rule approach. To establish a sum rule for the coupling constant, we will pick out the $1/q^2$ terms around the pole $q^2 \sim 0$ with the structure \not{p} in the OPE series and then match both sides of the sum rule. To apply sum rules appropriately, we shall calculated at Q^2 far away from the on-shell mass $-m_K^2$ to ensure the approximation $p^2 = p'^2 = P^2$ valid. After performing the Borel transform $P^2 \rightarrow M_B^2$ on both phenomenological and OPE sides, we obtain the strong coupling for $P_{ccs}\Xi_{cc}\bar{K}$ vertex

$$g_{P_{ccs}\Xi_{cc}\bar{K}}(s_0, M_B^2) = \frac{1}{\lambda_{P_{ccs}}^{-} \lambda_{\Xi_{cc}} \lambda_K (m_{P_{ccs}} + m_{\Xi_{cc}})} \frac{m_{P_{ccs}}^2 - m_{\Xi_{cc}}^2}{e^{-m_{\Xi_{cc}}^2/M_B^2} - e^{-m_{P_{ccs}}^2/M_B^2}} \left(\frac{Q^2 + m_K^2}{Q^2} \right) \left(\int_{s_{\leq}}^{s_0} ds \rho(s) e^{-s/M_B^2} + R(M_B^2) \right), \quad (13)$$

and strong coupling for $P_{ccs}\Omega_{cc}\pi$ vertex

$$g_{P_{ccs}\Omega_{cc}\pi}(s_0, M_B^2) = \frac{1}{\lambda_{P_{ccs}}^{-} \lambda_{\Omega_{cc}} \lambda_{\pi} (m_{P_{ccs}} + m_{\Omega_{cc}})} \frac{m_{P_{ccs}}^2 - m_{\Omega_{cc}}^2}{e^{-m_{\Omega_{cc}}^2/M_B^2} - e^{-m_{P_{ccs}}^2/M_B^2}} \left(\frac{Q^2 + m_{\pi}^2}{Q^2} \right) \left(\int_{s_{\leq}}^{s_0} ds \rho(s) e^{-s/M_B^2} + R(M_B^2) \right), \quad (14)$$

where the continuum threshold $s_0 = 22.3 \text{ GeV}^2$ is taken from the two-point mass sum rules in Ref. [39].

Using the operator product expansion (OPE) method, the three-point function can also be evaluated at the quark-gluonic level as a function of various QCD parameters. To evaluate the Wilson coefficients, we adopt the quark propagator in momentum space and the propagator

$$iS_Q^{ab}(p) = \frac{i\delta^{ab}}{\not{p} - m_Q} + \frac{i}{4}g_s \frac{\lambda_{ab}^n}{2} G_{\mu\nu}^n \frac{\sigma^{\mu\nu}(\not{p} + m_Q) + (\not{p} + m_Q)\sigma^{\mu\nu}}{(p^2 - m_Q^2)^2} + \frac{i\delta^{ab}}{12} \langle g_s^2 GG \rangle m_Q \frac{p^2 + m_Q \not{p}}{(p^2 - m_Q^2)^4}, \quad (15)$$

$$iS_q^{ab}(x) = \frac{i\delta^{ab}}{2\pi^2 x^4} \not{x} - \frac{\delta^{ab}}{12} \langle \bar{q}q \rangle + \frac{i}{32\pi^2} \frac{\lambda_{ab}^n}{2} g_s G_{\mu\nu}^n \frac{1}{x^2} (\sigma^{\mu\nu} \not{x} + \not{x} \sigma^{\mu\nu}) \\ + \frac{\delta^{ab} x^2}{192} \langle \bar{q}g_s \sigma \cdot Gq \rangle - \frac{m_q \delta^{ab}}{4\pi^2 x^2} + \frac{i\delta^{ab} m_q \langle \bar{q}q \rangle}{48} \not{x} - \frac{im_q \langle \bar{q}g_s \sigma \cdot Gq \rangle \delta^{ab} x^2 \not{x}}{1152}, \quad (16)$$

where Q represents the heavy quark c or b , q represents the light quark u, d, s , the superscripts a, b denote the color indices. In this work, we will evaluate Wilson coefficients of the correlation function up to dimension nine condensates at the leading order in α_s . The spectrum function $\rho(s)$ in Eqs. (13), (14) are given in Appendix A. We shall discuss the detail to obtain suitable parameter working regions in QCD sum rule analysis in next section.

III. NUMERICAL ANALYSIS

In this section we perform the three-point QCD sum rule analysis for double heavy molecular pentaquark systems using the interpolating currents in Eq. (2). We use the standard values of various QCD condensates as $\langle \bar{q}q \rangle(1\text{GeV}) = -(0.24 \pm 0.03)^3 \text{ GeV}^3$, $\langle \bar{q}g_s \sigma \cdot Gq \rangle(1\text{GeV}) = -M_0^2 \langle \bar{q}q \rangle$, $M_0^2 = (0.8 \pm 0.2) \text{ GeV}^2$, $\langle \bar{s}s \rangle / \langle \bar{q}q \rangle = 0.8 \pm 0.1$, $\langle g_s^2 GG \rangle(1\text{GeV}) = (0.48 \pm 0.14) \text{ GeV}^4$ at the energy scale $\mu = 1\text{GeV}$ [51, 55–61] and $m_s(2 \text{ GeV}) = 95_{-3}^{+9} \text{ MeV}$, $m_c(m_c) = 1.27_{-0.04}^{+0.03} \text{ GeV}$, $m_b(m_b) = 4.18_{-0.03}^{+0.04} \text{ GeV}$ from the Particle Data Group[62]. We also take into account the energy-scale dependence of the above parameters from the renormalization group equation [63]

$$m_s(\mu) = m_s(2\text{GeV}) \left[\frac{\alpha_s(\mu)}{\alpha_s(2\text{GeV})} \right]^{\frac{12}{33-2n_f}}, \\ m_c(\mu) = m_c(m_c) \left[\frac{\alpha_s(\mu)}{\alpha_s(m_c)} \right]^{\frac{12}{33-2n_f}}, \\ m_b(m_b) = m_b(m_b) \left[\frac{\alpha_s(\mu)}{\alpha_s(m_b)} \right]^{\frac{12}{33-2n_f}}, \\ \langle \bar{q}q \rangle(\mu) = \langle \bar{q}q \rangle(1\text{GeV}) \left[\frac{\alpha_s(1\text{GeV})}{\alpha_s(\mu)} \right]^{\frac{12}{33-2n_f}}, \\ \langle \bar{s}s \rangle(\mu) = \langle \bar{s}s \rangle(1\text{GeV}) \left[\frac{\alpha_s(1\text{GeV})}{\alpha_s(\mu)} \right]^{\frac{12}{33-2n_f}}, \\ \langle \bar{q}g_s \sigma \cdot Gq \rangle(\mu) = \langle \bar{q}g_s \sigma \cdot Gq \rangle(1\text{GeV}) \left[\frac{\alpha_s(1\text{GeV})}{\alpha_s(\mu)} \right]^{\frac{2}{33-2n_f}}, \\ \langle \bar{s}g_s \sigma \cdot Gs \rangle(\mu) = \langle \bar{s}g_s \sigma \cdot Gs \rangle(1\text{GeV}) \left[\frac{\alpha_s(1\text{GeV})}{\alpha_s(\mu)} \right]^{\frac{2}{33-2n_f}}, \\ \alpha_s(\mu) = \frac{1}{b_0 t} \left[1 - \frac{b_1}{b_0} \frac{\log t}{t} + \frac{b_1^2 (\log^2 t - \log t - 1) + b_0 b_2}{b_0^4 t^2} \right], \quad (17)$$

where $t = \log \frac{\mu^2}{\Lambda^2}$, $b_0 = \frac{33-2n_f}{12\pi}$, $b_1 = \frac{153-19n_f}{24\pi^2}$, $b_2 = \frac{2857 - \frac{5033}{9}n_f + \frac{325}{27}n_f^2}{128\pi^3}$, $\Lambda = 210 \text{ MeV}$, 292 MeV and 332 MeV for the flavors $n_f = 5, 4$ and 3 , respectively. In this work, we evolve all the input parameters to the energy scale $\mu = m_c$ for our sum rule analysis. The parameters for the K and π mesons and double charm baryons are adopted in Tab. I.

A. Strong coupling $g_{P_{ccs}\Xi_{cc}\bar{K}}$

In the left panel of Fig. 2, we show the variation of the coupling constant $g_{P_{ccs}\Xi_{cc}\bar{K}}(Q^2)$ with the Borel mass M_B^2 at $Q^2 = m_{\Xi_{cc}}^2 \sim 13.1 \text{ GeV}^2$. Such a momentum point is chosen far away from m_K^2 so that it can be safely ignored and the OPE series is

TABLE I: The values of the hadronic parameters m_H and f_H in the work taken from Refs. [62, 64–66].

Meson(M)	Mass m_M [GeV]	Decay constant f_M [GeV]	Baryon(B)	Mass m_B [GeV]	Decay constant f_B [GeV]
π	0.140	0.16 ± 0.04	Ξ_{cc}^{++}	3.621	0.109
K	0.494	0.16 ± 0.02	Ω_{cc}^+	3.738	0.138

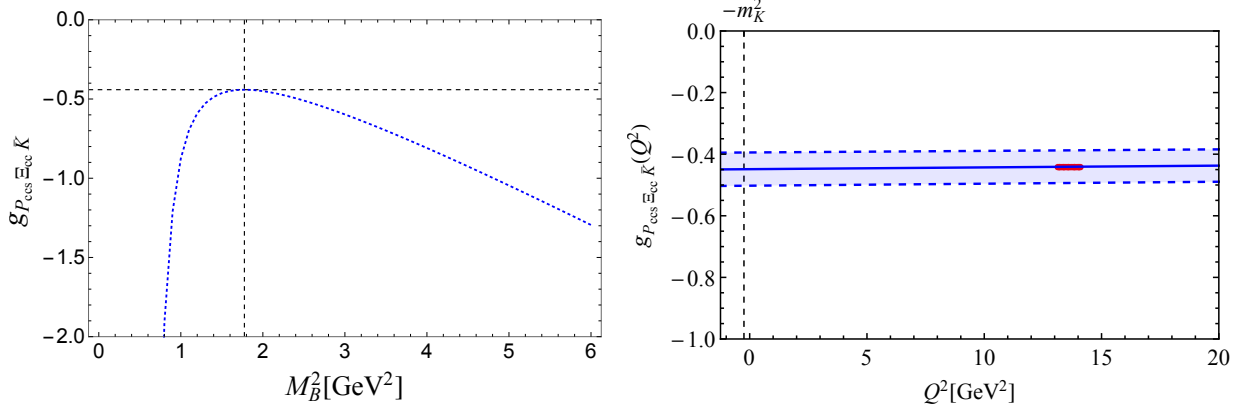


FIG. 2: The dependence of the strong coupling $g_{P_{ccs}\Xi_{cc}\bar{K}}$ on the Borel mass M_B^2 (left panel) and transfer momentum Q^2 (right panel). On the left panel, the transfer momentum is set to be $Q^2 = m_{\Xi_{cc}}^2 \sim 13.1$ GeV². On the right panel, the red dots denote the value from Eq. (13) with $s_0 = 22.3$ GeV² and $M_B^2 = 1.77$ GeV². The blue solid line is the exponential fitting curve. The two dashed blue lines denote the upper and lower boundary of the uncertainty from various condensates, quark masses and hadronic parameters.

valid in this region. We find that the coupling constant $g_{P_{ccs}\Xi_{cc}\bar{K}}(Q^2)$ has a maximum value at $M_B^2 \sim 1.77$ GeV², around which it has minimal dependence on the non-physical parameter M_B^2 . To extrapolate the coupling constant from the valid QCD sum rule working region to the physical pole $Q^2 = -m_K^2$, we fit the sum rule result for $s_0 = 22.3$ GeV² and $M_B^2 = 1.77$ GeV² with exponential model

$$g_{P_{ccs}\Xi_{cc}\bar{K}}(Q^2) = a e^{-b Q^2}. \quad (18)$$

The fitting curve is shown in the right panel of Fig. 2, and the result is as follow:

$$g_{P_{ccs}\Xi_{cc}\bar{K}}(Q^2) = -(0.449 \pm 0.054 \text{ GeV}^{-3}) e^{-(0.001 \pm 0.000) \text{ GeV}^{-2} Q^2}. \quad (19)$$

With the on-shell condition $Q^2 = -m_K^2$, we can obtain the strong coupling constant $g_{P_{ccs}\Xi_{cc}\bar{K}}(-m_K^2) = -(0.45 \pm 0.05) \text{ GeV}^2$. From the matrix element, we can obtain the decay width for $P_{ccs}^{++} \rightarrow \Xi_{cc}^{++} \bar{K}^0$ process:

$$\Gamma(P_{ccs}^{++} \rightarrow \Xi_{cc}^{++} \bar{K}^0) = \frac{\sqrt{\lambda(m_{P_{ccs}}^2, m_{\Xi_{cc}}^2, m_K^2)}}{8\pi m_{P_{ccs}}^2} g_{P_{ccs}\Xi_{cc}\bar{K}}(-m_K^2) ((m_{P_{ccs}} + m_{\Xi_{cc}})^2 - m_K^2). \quad (20)$$

Substitute the above on-shell coupling, we can obtain the decay width as

$$\Gamma(P_{ccs}^{++} \rightarrow \Xi_{cc}^{++} \bar{K}^0) = 65.02 \pm 15.69 \text{ MeV}. \quad (21)$$

B. Strong coupling $g_{P_{ccs}\Omega_{cc}\pi}$

As for $P_{ccs}\Omega_{cc}\pi$ process, in the left panel of Fig. 3, we show the variation of the coupling constant $g_{P_{ccs}\Omega_{cc}\pi}(Q^2)$ with the Borel mass M_B^2 at $Q^2 = m_{\Omega_{cc}}^2 \sim 13.8$ GeV². Such a momentum point is chosen far away from $m_{\pi^*}^2$ so that it can be safely ignored and the OPE series is valid in this region. We find that the coupling constant $g_{P_{ccs}\Omega_{cc}\pi}(Q^2)$ has a maximum value at $M_B^2 \sim 1.74$ GeV², around which it has minimal dependence on the non-physical parameter M_B^2 . We find that the results can be well fitted by the exponential model

$$g_{P_{ccs}\Omega_{cc}\pi}(Q^2) = a e^{-b Q^2}. \quad (22)$$

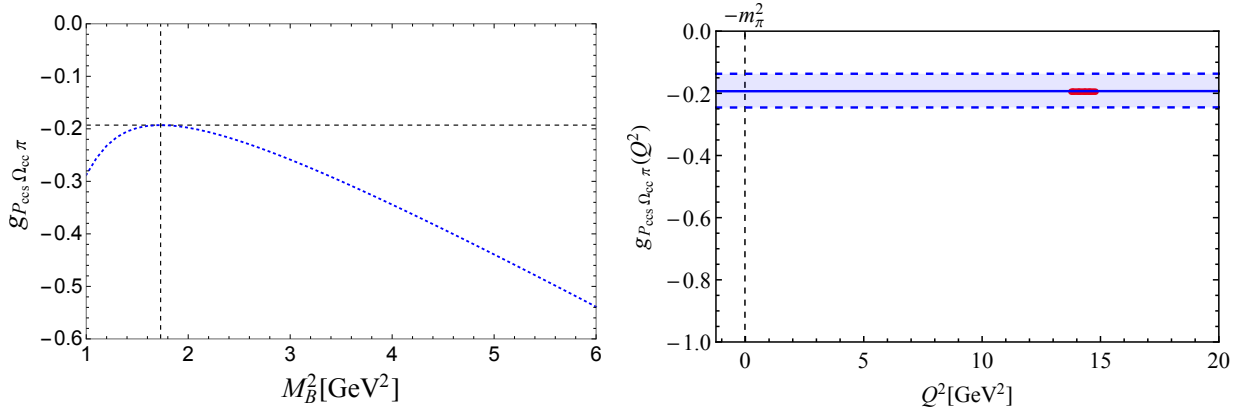


FIG. 3: The dependence of the strong coupling $g_{P_{ccs}\Omega_{cc}\pi}$ on the Borel mass M_B^2 (left panel) and transfer momentum Q^2 (right panel). On the left panel, the transfer momentum is set to be $Q^2 = m_{\Omega_{cc}}^2 \sim 13.8 \text{ GeV}^2$. On the right panel, the red dots denote the value from Eq. (14) with $s_0 = 22.3 \text{ GeV}^2$ and $M_B^2 = 1.74 \text{ GeV}^2$. The blue solid line is the exponential fitting curve. The two dashed blue lines denote the upper and lower boundary of the uncertainty from various condensates, quark masses and hadronic parameters.

The fitting curve is shown in the right panel of Fig. 3, and the result is as follow:

$$g_{P_{ccs}\Omega_{cc}\pi}(Q^2) = -(0.193^{+0.052}_{-0.056} \text{ GeV}^{-3})e^{-(0.000 \pm 0.00) \text{ GeV}^{-2} Q^2}. \quad (23)$$

With the on-shell condition $Q^2 = -m_\pi^2$, we can obtain the strong coupling constant $g_{P_{ccs}\Omega_{cc}\pi}(-m_\pi^2) = -0.193$. From the matrix element, we can obtain the decay width for $P_{ccs}^{++} \rightarrow \Xi_{cc}^{++} \bar{K}^0$ process:

$$\Gamma(P_{ccs}^{++} \rightarrow \Omega_{cc}^+ \pi^+) = \frac{\sqrt{\lambda(m_{P_{ccs}}^2, m_{\Omega_{cc}}^2, m_\pi^2)}}{8\pi m_{P_{ccs}}^2} g_{P_{ccs}\Omega_{cc}\pi}(-m_\pi^2) ((m_{P_{ccs}} + m_{\Omega_{cc}})^2 - m_\pi^2). \quad (24)$$

Substitute the above on-shell coupling, we can obtain the decay width as

$$\Gamma(P_{ccs}^{++} \rightarrow \Omega_{cc}^+ \pi^+) = 19.56^{+11.15}_{-10.36} \text{ MeV}. \quad (25)$$

Thus, we can obtain the total strong decay width as

$$\begin{aligned} \Gamma_{P_{ccs}^{++}} &= \Gamma(P_{ccs}^{++} \rightarrow \Xi_{cc}^{++} \bar{K}^0) + \Gamma(P_{ccs}^{++} \rightarrow \Omega_{cc}^+ \pi^+) \\ &= (84.58^{+19.25}_{-18.80}) \text{ MeV}. \end{aligned} \quad (26)$$

IV. PRODUCTION VIA FINAL-STATE-INTERACTION

In the framework of rescattering mechanism, the decay $\Xi_{bc}^+ \rightarrow P_{ccs}^{++} D^-$ can most likely proceed as $\Xi_{bc}^+ \rightarrow D_s^{*-} \Xi_{cc}^{++} \rightarrow D^- P_{ccs}^{++}$ with K^0 exchange. Under the factorization approach [67–69], we can get the decay amplitude of $\Xi_{bc}^+ \rightarrow D_s^* \Xi_{cc}$:

$$\mathcal{A}(\Xi_{bc}^+ \rightarrow D_s^* \Xi_{cc}) = \frac{G_F}{\sqrt{2}} V_{cb} V_{cs} a_1 \epsilon^{*\mu} \bar{u}_{\Xi_{cc}} \left(A_1 \gamma_\mu \gamma_5 + A_2 \frac{p_{\Xi_{cc}}^\mu}{m_{\Xi_{bc}}} \gamma_5 + B_1 \gamma_\mu + B_2 \frac{p_{\Xi_{cc}}^\mu}{m_{\Xi_{bc}}} \right). \quad (27)$$

The above decay amplitudes in the factorization approach are expressed as

$$A_1 = -\lambda_{D_s^*} \left[g_1(m_{D_s^*}^2) + g_2(m_{D_s^*}^2) \frac{m_{\Xi_{cc}} - m_{\Xi_{bc}}}{m_{\Xi_{bc}}} \right], \quad (28)$$

$$A_2 = -2\lambda_{D_s^*} g_2(m_{D_s^*}^2), \quad (29)$$

$$B_1 = \lambda_{D_s^*} \left[f_1(m_{D_s^*}^2) - f_2(m_{D_s^*}^2) \frac{m_{\Xi_{cc}} + m_{\Xi_{bc}}}{m_{\Xi_{bc}}} \right], \quad (30)$$

$$B_2 = 2\lambda_{D_s^*} f_2(m_{D_s^*}^2), \quad (31)$$

where G_F is the Fermi constant, V_{ik} is the CKM matrix elements, a_1 is the effective Wilson coefficients obtained by the factorization approach [70], and $f_{1,2}$ and $g_{1,2}$ are transition form factors of $\Xi_{bc}^+ \rightarrow \Xi_{cc}^* D_s^*$ weak decay process. The above form factors can be parametrized as

$$F(Q^2) = \frac{F(0)}{1 - \frac{Q^2}{m_{\text{fit}}^2} + \delta \left(\frac{Q^2}{m_{\text{fit}}^2} \right)^2}, \quad (32)$$

where the parameters F_0 , m_{fit} and δ are taken in Ref. [69] and listed in Tab. II. The amplitude for $\Xi_{bc}^+ \rightarrow D_s^{*-} \Xi_{cc}^{++} \rightarrow D^- P_{ccs}^{++}$

TABLE II: The values of the parameters $F(0)$, m_{fit} and δ for the form factors in Eqs. (28)-(31) for $\Xi_{bc}^+ \rightarrow D_s^{*-} \Xi_{cc}^{++}$ process taken from Ref. [69].

Form Factor	$F(0)$	m_{fit}	δ	Form Factor	$F(0)$	m_{fit}	δ
f_1	0.550	4.45	0.43	g_1	0.530	4.57	0.44
f_2	-0.230	4.07	0.47	g_2	-0.043	3.90	0.48

process can be written as:

$$\begin{aligned} & \mathcal{A}(\Xi_{bc}^+ \rightarrow D_s^{*-} \Xi_{cc}^{++} \rightarrow D^- P_{ccs}^{++}) \\ &= i \frac{G_F}{\sqrt{2}} V_{cb} V_{cs} a_1 \int_{-1}^1 \frac{|p_{D_s^*}| d\cos\theta d\phi}{32\pi^2 m_{\Xi_{bc}}^2 m_{D_s^*}^2} \frac{g_{D_s^* DK}(-t) g_{P_{ccs} \Xi_{cc} \bar{K}}(-t)}{t - m_K^2} \bar{u}_{P_{ccs}}(p_P, s_P) (\not{p}_{\Xi_{cc}} + m_{\Xi_{cc}}) H u_{\Xi_{bc}}(p_{\Xi_{bc}}, s_{\Xi_{bc}}), \end{aligned} \quad (33)$$

where

$$H = -(p_D \cdot p_{D_s^*}) (m_{\Xi_{bc}} \not{p}_{D_s^*} (A_1 \gamma_5 + B_1) + p_{D_s^*} \cdot p_{\Xi_{cc}} (A_2 \gamma_5 + B_2)) + m_{D_s^*}^2 (m_{\Xi_{bc}} \not{p}_D (A_1 \gamma_5 + B_1) + p_D \cdot p_{\Xi_{cc}} (A_2 \gamma_5 + B_2)). \quad (34)$$

The corresponding decay width can be written as

$$\Gamma(\Xi_{bc}^+ \rightarrow P_{ccs}^{++} D^-) = \frac{\sqrt{\lambda(m_{\Xi_{bc}}^2, m_D^2, m_{P_{ccs}}^2)}}{16\pi m_{\Xi_{bc}}^3} |\mathcal{A}(\Xi_{bc}^+ \rightarrow D_s^{*-} \Xi_{cc}^{++} \rightarrow D^- P_{ccs}^{++})|^2. \quad (35)$$

It should be noted that in some work of final state interaction formalism [45, 47], the decay amplitude contains the form factor $F(t, m) = (\Lambda^2 - m_K^2)/(\Lambda^2 - t)$ for each strong vertices, which is introduced to compensate the off-shell effect of the exchanged particle at the vertices [71]. In this work, we can contain the off-shell effect with Q^2 -dependent strong coupling, such as $g_{D_s^* DK}(Q^2)$ and $g_{P_{ccs} \Xi_{cc} \bar{K}}(Q^2)$. We take the result of strong coupling $g_{D_s^* DK}(Q^2)$ with QCD sum rule formalism as follow [46]:

$$g_{D_s^* DK}(Q^2) = (2.82_{-0.82}^{+1.34} \text{ GeV}^{-2}) e^{-(0.22 \pm 0.00 \text{ GeV}^{-2}) Q^2}. \quad (36)$$

With strong coupling Eqs. (19), (36) and Eq. (35), and the mass of Ξ_{bc}^+ taken from the lattice result [64], the decay width of $\Xi_{bc}^+ \rightarrow P_{ccs}^{++} D^-$ process can be calculated as

$$\Gamma(\Xi_{bc}^+ \rightarrow P_{ccs}^{++} D^-) = (1.17_{-0.40}^{+0.55}) \times 10^{-17} \text{ GeV}. \quad (37)$$

We take the lattice result of lifetime of Ξ_{bc}^+ [64], the production branching fraction of $\Xi_{bc}^+ \rightarrow P_{ccs}^{++} D^-$ process can be calculate as

$$\mathcal{Br}(\Xi_{bc}^+ \rightarrow P_{ccs}^{++} D^-) = (4.32_{-1.47}^{+2.02}) \times 10^{-6}. \quad (38)$$

V. SUMMARY

Based on our previous calculations of mass spectroscopy [39], we further study the decay and production properties of the exotic strange double charm pentaquark state P_{ccs}^{++} with $J^P = 1/2^-$. We perform the three-point QCD sum rules to calculate the coupling constants of $P_{ccs}^{++} \rightarrow \Xi_{cc}^{++} \bar{K}^0$ and $P_{ccs}^{++} \rightarrow \Omega_{cc}^+ \pi^+$ strong decay processes. The partial decay widths of these two process are obtained as

$$\begin{aligned} \Gamma(P_{ccs}^{++} \rightarrow \Xi_{cc}^{++} \bar{K}^0) &= 65.02 \pm 15.69 \text{ MeV}, \\ \Gamma(P_{ccs}^{++} \rightarrow \Omega_{cc}^+ \pi^+) &= 19.56_{-10.36}^{+11.15} \text{ MeV}, \end{aligned} \quad (39)$$

yielding a relative branching ratio $\Gamma(P_{ccs}^{++} \rightarrow \Xi_{cc}^{++} \bar{K}^0) : \Gamma(P_{ccs}^{++} \rightarrow \Omega_{cc}^+ \pi^+) \approx 3.3 : 1$. The total decay width is predicted as

$$\Gamma_{P_{ccs}^{++}} = 84.58_{-18.80}^{+19.25} \text{ MeV}. \quad (40)$$

Furthermore, we study the $\Xi_{bc}^+ \rightarrow D_s^- \Xi_{cc}^{++} \rightarrow D^- P_{ccs}^{++}$ process via the rescattering mechanism to estimate the branching ratio of $\Xi_{bc}^+ \rightarrow D^- P_{ccs}^{++}$ as $(4.32_{-1.47}^{+2.02}) \times 10^{-6}$. This value of branching ratio aligns with the productions of hidden-charm pentaquark states in Ξ_b decays [72–74] (with a same $b \rightarrow c\bar{c}s$ weak transitions), which typically around $\mathcal{B}r \sim 10^{-6} - 10^{-5}$. Combining with the decay branching ratio $\mathcal{B}r(P_{ccs}^{++} \rightarrow \Xi_{cc}^{++} \bar{K}^0)$, we obtain $\mathcal{B}r(\Xi_{bc}^+ \rightarrow D^- P_{ccs}^{++} \rightarrow D^- \bar{K}^0 \Xi_{cc}^{++}) \approx \mathcal{B}r(\Xi_{bc}^+ \rightarrow D^- P_{ccs}^{++}) \mathcal{B}r(P_{ccs}^{++} \rightarrow \Xi_{cc}^{++} \bar{K}^0) = 3.3 \times 10^{-6}$, providing a benchmark for future experiments.

To date, LHCb has pursued Ξ_{bc}^+ state in $\Lambda_c \pi$, $\Xi_c \pi$ and DKp final states without significant signals [75–77]. Nevertheless, high Ξ_{bc}^+ yields have been expected at future facilities such as MuIC ($\sim 10^8$ events/year) [78], CEPC/FCC-ee ($\sim 10^7$ events/year) [79], LHeC ($\sim 10^5$ events/year) [80], and LHCb Run 3 ($\sim 10^4$ events/year) [81], producing a considerable amount of double charm pentaquark states in the future.

ACKNOWLEDGMENTS

This work is supported by the National Natural Science Foundation of China with Grant Nos. 12175318, the Natural Science Foundation of Guangdong Province of China under Grant No. 2022A1515011922.

Appendix A: Spectrum function for three-point correlation of strong vertices

The spectrum function $\rho(s)$ and $R(M_B^2)$ in Eq. (13) is shown as follow

$$\rho(s) = \int_{x_{\min}}^{x_{\max}} dx \int_{y_{\min}}^{y_{\max}} dy \frac{3}{512\pi^5} y (\pi^2 \langle GG \rangle m_s (2\langle \bar{q}q \rangle - \langle \bar{s}s \rangle) ((x-2)y+1) - \frac{x}{y-1} (\langle GG \rangle + 16\pi^2 m_s (\langle \bar{s}s \rangle - 2\langle \bar{q}q \rangle))) \Delta(x, y, s) (3(x-1)\Delta(x, y, s) + m_c^2 + 2s(x-1)(y-1)y), \quad (A1)$$

$$R(M_B^2) = \int_0^1 dx \int_0^1 dy \frac{\langle GG \rangle m_s (\langle \bar{s}s \rangle - 2\langle \bar{q}q \rangle) ((x-2)y+1)}{512\pi^3 (x-1)^2 (y-1)^2} (s_1(x-1)^2(y-1)^2 y - m_c^2(x(y(4((x-1)x+1)y-2x-5)+3) + y-1)) e^{-s_1/M_B^2}, \quad (A2)$$

where $x_{\min} = 0$, $x_{\max} = \frac{1-2\sqrt{m_c^2/s}}{(1-\sqrt{m_c^2/s})^2}$, $y_{\min} = \frac{s(1-x)+m_c^2x-\sqrt{(s(1-x)+m_c^2x)^2-4m_c^2s(1-x)}}{2s(1-x)}$, $y_{\max} = \frac{s(1-x)+m_c^2x+\sqrt{(s(1-x)+m_c^2x)^2-4m_c^2s(1-x)}}{2s(1-x)}$, $\Delta(x, y, s) = -s(1-y)y + \frac{m_c^2(1-xy)}{1-x}$, $s_1 = \frac{m_c^2(1-xy)}{(1-x)(1-y)y}$.

The spectrum function $\rho(s)$ and $R(M_B^2)$ in Eq. (14) is shown as follow

$$\rho(s) = \int_{x_{\min}}^{x_{\max}} dx \int_{y_{\min}}^{y_{\max}} dy \frac{3}{512\pi^5 (y-1)} \langle GG \rangle xy \Delta(x, y, s) (-3(x-1)\Delta(x, y, s) - m_c^2 - 2s(x-1)(y-1)y) + \int_{z_{\min}}^{z_{\max}} dz \frac{3\langle GG \rangle m_s \langle \bar{s}s \rangle (z-1)}{128\pi^3} \quad (A3)$$

$$R(M_B^2) = \int_0^1 dz \frac{\langle GG \rangle m_s \langle \bar{s}s \rangle}{256\pi^3 z} (m_c^2 z - s_2(4z^2 - 6z + 2)) e^{-s_2/M_B^2} \quad (A4)$$

where $z_{\min} = \frac{1}{2} (1 - \sqrt{1 - 4m_c^2/s})$, $z_{\max} = \frac{1}{2} (1 + \sqrt{1 - 4m_c^2/s})$, and $s_2 = \frac{m_c^2}{(1-z)z}$.

-
- [1] M. Gell-Mann, Phys. Lett. **8**, 214 (1964)
 - [2] G. Zweig, in: D.Lichtenberg, S.P.Rosen(Eds.), Developments in the Quark Theory of Hadrons, VOL. 1. 1964 - 1978:pp. 22–101, 1964.
 - [3] M. Nielsen, F.S. Navarra, S.H. and Lee, Phys. Rept. **497**, 41 (2010)
 - [4] H. X. Chen, W. Chen, X. Liu and S. L. Zhu, Phys. Rept. **639**, 1-121 (2016)
 - [5] J.-M. Richard, Few Body Syst. **57**, 1185 (2016)
 - [6] A. Esposito, A. Pilloni and A. D. Polosa, Phys. Rept. **668**, 1-97 (2017)

- [7] A. Ali, J.S. Lange, and S. Stone, *Prog. Part. Nucl. Phys.* **97**, 123 (2017)
- [8] F. K. Guo, C. Hanhart, U. G. Meißner, Q. Wang, Q. Zhao and B. S. Zou, *Rev. Mod. Phys.* **90**, no.1, 015004 (2018)
- [9] R.M. Albuquerque, J.M. Dias, K.P. Khemchandani, A.M. Torres, F.S. Navarra, M. Nielsen, and C.M. Zanetti, *J. Phys. G* **46**, 093002 (2019)
- [10] Y. R. Liu, H. X. Chen, W. Chen, X. Liu and S. L. Zhu, *Prog. Part. Nucl. Phys.* **107**, 237-320 (2019)
- [11] N. Brambilla, S. Eidelman, C. Hanhart, A. Nefediev, C. P. Shen, C. E. Thomas, A. Vairo and C. Z. Yuan, *Phys. Rept.* **873**, 1-154 (2020)
- [12] J.-M. Richard, A. Valcarce, and J. Vijande, *Annals Phys.* **412**, 168009 (2020)
- [13] R.N. Faustov, V.O. Galkin, and E.M. Savchenko, *Universe* **7**, 94 (2021)
- [14] H. X. Chen, W. Chen, X. Liu, Y. R. Liu and S. L. Zhu, *Rept. Prog. Phys.* **86**, 026201 (2023)
- [15] L. Meng, B. Wang, G. J. Wang and S. L. Zhu, *Phys.Rept.* **1019** 1-149 (2023)
- [16] R. Aaij *et al.* [LHCb], *Phys. Rev. Lett.* **115**, 072001 (2015)
- [17] R. Aaij *et al.* [LHCb], *Nature Commun.* **13**, no.1, 3351 (2022)
- [18] R. Aaij *et al.* [LHCb], *Nature Phys.* **18**, no.7, 751-754 (2022)
- [19] R. Aaij *et al.* [LHCb], *Phys.Rev.D* **108**, 012017 (2023)
- [20] M.-J. Yan, X.-H. Liu, S. González-Solís, F.-K. Guo, C. Hanhart, U.-G. Meißner, and B.-S. Zou, *Phys. Rev. D* **98**, no.9, 091502 (2018)
- [21] X.-K. Dong, F.-K. Guo, and B.-S. Zou, *Commun. Theor. Phys.* **73**, no.12, 125201 (2021)
- [22] R. Chen, A. Hosaka, and X. Liu, *Phys. Rev. D* **96**, 116012 (2017)
- [23] Z.-H. Guo, *Phys. Rev. D* **96**, 074004 (2017)
- [24] R. Zhu, X. Liu, H. Huang, and C.-F. Qiao, *Phys. Lett. B* **797**, 134869 (2019)
- [25] B. Wang, K. Chen, L. Meng, and S.-L. Zhu, *Phys.Rev.D* **109**, 074035 (2024)
- [26] F.-B. Duan, Q.-N. Wang, Z.-Y. Yang, X.-L. Chen, and W. Chen, *Phys. Rev. D* **109**, 094018 (2024)
- [27] F. L. Wang and X. Liu, *Phys. Rev. D* **108**, no.7, 074022 (2023)
- [28] F. L. Wang and X. Liu, *Phys. Rev. D* **109**, no.1, 1 (2024)
- [29] L. C. Sheng, J. Y. Huo, R. Chen, F. L. Wang and X. Liu, *Phys. Rev. D* **110**, no.5, 054044 (2024)
- [30] R. Chen, N. Li, Z.-F. Sun, X. Liu, and S.-L. Zhu, *Phys. Lett. B* **822**, 136693 (2021)
- [31] Y. Xing, and Y. Niu, *Eur. Phys. J. C* **81**, 978 (2021)
- [32] Q.-S. Zhou, K. Chen, X. Liu, Y.-R. Liu, and S.-L. Zhu, *Phys. Rev. C* **98**, 045204 (2018)
- [33] Z.-G. Wang, *Eur. Phys. J. C* **78**, 826 (2018)
- [34] W. Park, S. Cho, and S. H. Lee, *Phys. Rev. D* **99**, 094023 (2019)
- [35] U. Özdem, *Eur. Phys. J. Plus* **137**, 936 (2022)
- [36] U. Özdem, *Eur. Phys. J. A* **61**, 10 (2025)
- [37] H. Y. Zhou, F. L. Wang, Z. W. Liu and X. Liu, *Phys. Rev. D* **106**, no.3, 034034 (2022)
- [38] S. H. Zhu, F. L. Wang and X. Liu, [arXiv:2510.18492 [hep-ph]].
- [39] Z.-Y. Yang, Q. Wang, and W. Chen, *Phys. Rev. D* **110**, 056022 (2024)
- [40] J.-W. Li, M.-Z. Yang, and D.-S. Du, *HEPNP* **27**, 665-672 (2003)
- [41] H.-Y. Cheng, C.-K. Chua, and A. Soni, *Phys. Rev. D* **71**, 014030 (2005)
- [42] C.-D. Lü, Y.-L. Shen, and W. Wang, *Phys. Rev. D* **73**, 034005 (2006)
- [43] J.-J. Han, H.-Y. Jiang, W. Liu, Z.-J. Xiao, and F.-S. Yu, *Chin. Phys. C* **45**, 053105 (2021)
- [44] C.-P. Jia, H.-Y. Jiang, J.-P. Wang, and F.-S. Yu, *JHEP* **11**, 072 (2024)
- [45] Y.-K. Chen, J.-J. Han, Q.-F. Lü, J.-P. Wang, and F.-S. Yu, *Eur. Phys. J. C* **81**, no.1, 71 (2021)
- [46] Z.-Y. Yang, Q. Wang, and W. Chen, *Phys. Rev. D* **111**, 076030 (2025)
- [47] Y.-K. Hsiao, S.-T. Cai, and Y.-L. Wang, *Phys. Rev. D* **111**, 7 (2025)
- [48] L. J. Reinders, H. Rubinstein, and S. Yazaki, *Phys. Rep.* **127**, 1 (1985)
- [49] M. A. Shifman, A. I. Vainshtein, and V. I. Zakharov, *Nucl. Phys.* **B147**, 385 (1979)
- [50] P. Colangelo and A. Khodjamirian, *At the Frontier of Particle Physics*, edited by M. Shifman (World Scientific, Singapore, 2001), Vol. **3**, pp. 1495–1576
- [51] S. Narison, *Camb. Monogr. Part. Phys. Nucl. Phys. Cosmol.* **17**, 1-812 (2007) Cambridge University Press, 2022, ISBN 978-1-00-929029-6, 978-1-00-929031-9, 978-1-00-929033-3, 978-0-521-03731-0, 978-0-521-81164-4, 978-0-511-18948-7
- [52] J.-R. Zhang, and M.-Q. Huang, *Chin. Phys. C* **33**, 1385 (2009)
- [53] B.S. Zou and F. Hussain, *Phys. Rev. C* **67**, 015204 (2003)
- [54] S. Narison, *Nucl. Part. Phys. Proc.*, **324-329**, 94 (2023).
- [55] M. Jamin, J. A. Oller, and A. Pich, *Eur. Phys. J. C* **24**, 237 (2002)
- [56] M. Jamin and A. Pich, *Nucl. Phys. B Proc. Suppl.* **74**, 300 (1999)
- [57] B. L. Ioffe, *Nucl. Phys.* **B188**, 317 (1981), [Erratum: *Nucl.Phys.B* **191**, 591–592 (1981)]
- [58] Y. Chung, H. G. Dosch, M. Kremer, and D. Schall, *Z. Phys. C* **25**, 151 (1984)
- [59] H. G. Dosch, M. Jamin, and S. Narison, *Phys. Lett. B* **220**, 251 (1989)
- [60] A. Khodjamirian, T. Mannel, N. Offen, and Y. M. Wang, *Phys. Rev. D* **83**, 094031 (2011)
- [61] A. Francis, R. J. Hudspith, R. Lewis, and K. Maltman, *Phys. Rev. D* **99**, 054505 (2019)
- [62] R. L. Workman *et al.* [Particle Data Group], *PTEP* **2022**, 083C01 (2022)
- [63] Z.-G. Wang, *Front.Phys.* **21**, 016300 (2026)
- [64] Z.S. Brown, W. Detmold, S. Meinel, and K. Orginos, *Phys. Rev. D* **90**, 094507 (2014)
- [65] Z.-G. Wang, *Eur. Phys. J. A* **45**, 267 (2010)
- [66] Y.-J. Shi, W. Wang, and Z.-X. Zhao, *Eur. Phys. J. C* **80** no.6, 568 (2020)
- [67] M. Wirbel, B. Stech, and M. Bauer, *Z. Phys. C* **29**, 637 (1985)

- [68] M. Bauer, B. Stech, and M. Wirbel, Z. Phys. C **34**, 103 (1987)
- [69] W. Wang, F.-S. Yu, and Z.-X. Zhao, Eur. Phys. J. C **77**, 781 (2017)
- [70] G. Buchalla, A.J. Buras, and M.E. Lautenbacher, Rev. Mod. Phys. **68**, 1125-1144 (1996)
- [71] O. Gortchakov, M.P. Locher, V.E. Markushin, and S. von Rotz, Z. Phys. A **353**, 447 (1996)
- [72] Q. Wu, D.-Y. Chen, and R. Ji, Chin. Phys. Lett. **38** no.7, 071301 (2021)
- [73] Y.-W. Pan, M.-Z. Liu, and L.-S. Geng, Phys. Rev. D **108** no.11, 114022 (2023)
- [74] Q. Wu, and D.-Y. Chen, Phys. Rev. D **109** no.9, 094003 (2024)
- [75] R. Aaij *et al.* [LHCb], JHEP **11**, 095 (2020)
- [76] R. Aaij *et al.* [LHCb], Chin. Phys. C **45** no.9, 093002 (2021)
- [77] R. Aaij *et al.* [LHCb], Chin. Phys. C **47** no.9, 093001 (2023)
- [78] X.-Y. Zhao, L. Guo, X.-C. Zheng, H.-Y. Bi, X.-G. Wu, and Q.-W. Ke, Chin. Phys. C **49** no.5, 053103 (2025)
- [79] H.-H. Ma, J.-J. Niu, and L. Guo, JHEP **05**, 197 (2025)
- [80] H.-Y. Bi, R.-Y. Zhang, X.-G. Wu, W.-G. Ma, X.-Z. Li, and S. Owusu, Phys. Rev. D **95** no.7, 074020 (2017)
- [81] P.-H. Zhang, L. Guo, X.-C. Zheng, and Q.-W. Ke, Phys. Rev. D **105**, 034016 (2022)